Engineering Analysis with Boundary Elements 119 (2020) 183–188

Contents lists available at ScienceDirect

Engineering Analysis with Boundary Elements

journal homepage: www.elsevier.com/locate/enganabound

Lubrication problems solved by the boundary element method

Massimo Guiggiani

Dipartimento di Ingegneria Civile e Industriale, Università di Pisa, Largo Lucio Lazzarino 1, 56122 Pisa PI, Italy

ARTICLE INFO

Keywords:
lubrication
BEM
Fundamental solution

ABSTRACT

A boundary element method (BEM) for the solution of lubrication problems on finite bearings is presented. The formulation requires the Reynolds equation to be transformed into a constant coefficient equation. Several film shapes that make the transformation possible are systematically obtained. Noticeably, they cover most practical cases. As an example of application, a numerical solution that only requires the discretization of the boundary is presented for a finite pad bearing.

1. Introduction

The solution of lubrication problems for finite bearings often rely on numerical methods, as analytical or semianalytical methods are fairly restrictive [1,2]. The most widely used numerical techniques for the solution of the Reynolds equation in two dimensions are the finite difference method (FDM) and the finite element method (FEM) (e.g. [3,4]). However, both methods require the discretization of the *whole* bearing pad.

The boundary element method (BEM), which is based on the formulation of the original problem in terms of integral equations, is now established as a powerful computational tool for many different fields of applied mechanics (e.g. [5,6]). The most distinctive feature of the BEM is that it only requires the discretization of the *contour* of the region under consideration, with obvious advantages over the FDM and FEM. Moreover, BEM solutions generally show very high accuracy, as they exactly satisfy the governing differential equation at all interior points.

Unfortunately, the application range of the BEM is generally confined to problems governed by partial differential equations with *constant* coefficients, which, in general, is not the case of Reynolds equation for self-acting films (e.g. hydrodynamic slider bearings). For linear elliptic equations with variable coefficients it is often possible to obtain the relevant integral equation (the first step in any BEM analysis), but in most cases the corresponding *fundamental solution* (the second key ingredient) is not known [7].

This fact probably accounts for the very limited application of the BEM to the solution of lubrication problems. In [8,9], two-dimensional steady viscous flows leading to a biharmonic equation for the stream function are considered. In [10] externally pressurized films with constant thickness, whose analysis requires the solution of the Laplace equation, are studied. Since the biharmonic and Laplace equations have constant coefficients, BEM procedures are quite well established. Only in [11] a self-acting hydrodynamic slider bearing was analysed. However, the lack of a fundamental solution for the general Reynolds equation led to a numerical method that required both boundary elements *and* internal cells. Moreover, as the internal cells involved the *unknown* pressure, an iterative solution procedure had to be used. Thus, most of the advantages of BEM were lost.

More recent contributions on the application of boundary element techniques to lubrication problems can be found in [12–15]. However, in [12–14] the BEM is only applied to solve the elasticity problem. In [15] it is acknowledged that the solution of the hydrodynamic model exclusively by BEM is not chosen for convenience, thus avoiding the mathematical treatment of non self-adjoint terms.

In the present paper it is shown, indeed, how the Reynolds equation for finite pad bearings can be manipulated to obtain a form more amenable for the application of a true BEM algorithm. Different bearing geometries that allow the Reynolds equation to be transformed into an equivalent differential equation, but with *constant* coefficients, are systematically obtained.

Thus, advanced BEM implementations are now possible also for hydrodynamic lubrication problems.

2. Statement of the problem

Let Ω be a finite region of the xy plane with boundary Γ as shown in Fig. 1. The steady state incompressible lubrication problem for sliding bearings in two dimensions is governed by the following form of the Reynolds equation, for $(x, y) \in \Omega$ (e.g. [2, p. 56] or [4, p. 80])

$$\frac{\partial}{\partial x}\left(h^3 \frac{\partial p}{\partial x}\right) + \frac{\partial}{\partial y}\left(h^3 \frac{\partial p}{\partial y}\right) = 6\mu U \frac{\partial h}{\partial x} \tag{1}$$

where the lubricant viscosity μ has been considered constant throughout the bearing. In (1), all symbols have their usual meaning, that is $p = p(x, y)$ is the lubricant pressure, $h = h(x, y) > 0$ is the film thickness, and

E-mail address: massimo.guiggiani@unipi.it

https://doi.org/10.1016/j.enganabound.2020.07.011
Received 12 May 2020; Received in revised form 14 July 2020; Accepted 15 July 2020

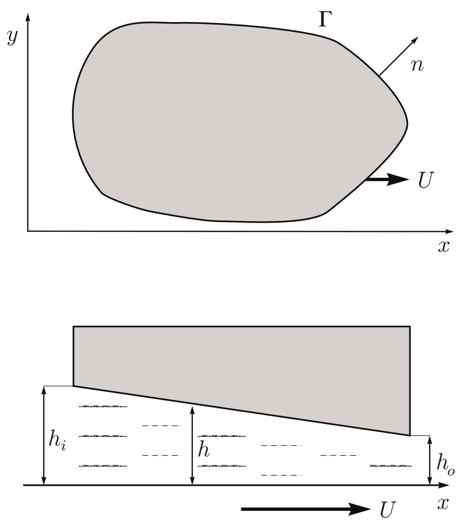

Fig. 1. Pad bearing configuration.

U is the velocity (assumed parallel to the x axis) of the driving surface (Fig. 1). For simplicity, no squeeze film terms have been considered.

The boundary conditions associated with (1), in general, are of the following types

$$p = \bar{p}, \quad \text{on } \Gamma_1 \tag{2}$$

$$\partial p/\partial n = \bar{q}, \quad \text{on } \Gamma_2 \tag{3}$$

where n denotes the outward normal to $\Gamma = \Gamma_1 \cup \Gamma_2$ (Fig. 1).

For a BEM treatment to be possible, it is convenient to introduce a new unknown function $\mathcal{P}(x, y)$

$$\mathcal{P} = p h^{3/2} \tag{4}$$

thus obtaining the following alternative form of the Reynolds equation

$$\nabla^2 \mathcal{P} - \frac{\nabla^2 (h^{3/2})}{h^{3/2}} \mathcal{P} = \frac{6\mu U}{h^{3/2}} \frac{\partial h}{\partial x} \tag{5}$$

or, more concisely

$$\nabla^2 \mathcal{P} + f(x, y)\mathcal{P} = g(x, y) \tag{6}$$

where $\nabla^2 = (\partial^2/\partial x^2 + \partial^2/\partial y^2)$ is the Laplacian operator, and $f(x, y)$ and $g(x, y)$ are known functions.

Note that the transformation (4) also affects the boundary conditions (2) and (3) which become, respectively

$$\mathcal{P} = \bar{p} h^{3/2}, \quad \text{on } \Gamma_1 \tag{7}$$

$$\frac{\partial \mathcal{P}}{\partial n} - \frac{3\mathcal{P}}{2h} \frac{\partial h}{\partial n} = \bar{q} h^{3/2}, \quad \text{on } \Gamma_2 \tag{8}$$

However, the transformed boundary conditions are still linear, and in the very common case $\bar{q} = 0$ and $\partial h/\partial n = 0$ on Γ_2, condition (8) simply turns out to be $\partial \mathcal{P}/\partial n = 0$.

Although Eq. (6) (or (5)) is fully equivalent to the original Eq. (1), it is more suitable for a BEM analysis, as it does not contain first partial derivatives of the unknown function $\mathcal{P}(x, y)$.

The use of transformation (4) in the context of lubrication apparently dates back to 1937, as reported in [2, pp. 74–75], though for completely different purposes. In the BEM literature, it is considered in [16] for Darcy's flow with variable permeability and in [17] in the context of generalized Laplace equations.

For a full BEM treatment to be possible it remains to determine the conditions for which (6) has *constant coefficients*, that is for which $f(x, y) = \text{constant}$.

3. Special film shapes

It is well known in hydrodynamic lubrication theory that, once the inlet and outlet film thicknesses are specified (Fig. 1), the exact shape of the oil film is not of great significance, as it does not markedly influence the performance of pad bearings [1, pp. 122–124], [18, pp. 60–62], [19]. Thus, the film shape can be chosen for mathematical convenience.

This conclusion holds for two-dimensional problems as well (e.g. [1, p. 59]). Therefore, the film shape $h(x, y)$ can be chosen in (5) and (6) in such a way to satisfy $f(x, y) = k$, that is

$$\nabla^2 (h^{3/2}) + k h^{3/2} = 0 \tag{9}$$

where k is a (real) constant to be fixed.

The homogeneous partial differential Eq. (9) in the unknown function $w = h^{3/2}$ is of fundamental importance as it defines *all* film shapes that transform (6) (or (5)) into the *constant coefficient* equation

$$\nabla^2 \mathcal{P} + k\mathcal{P} = g(x, y) \tag{10}$$

Eq. (10) is, indeed, three different equations, depending on whether k is greater than, less than, or equal to zero. For all cases the corresponding *fundamental solutions* are known (e.g. [17, Eqs. (11)–(13)]), and the BEM is easily applicable.

The problem is now reduced to the search of solutions for the homogeneous partial differential Eq. (9) in $w = h^{3/2}$. As already mentioned, the cases $k = \lambda^2$, $k = 0$, and $k = -\lambda^2$ (with $\lambda \neq 0$) have to be considered separately, as they give rise to different types of differential equations.

The particular case $h = h(x)$ will also be considered in detail, as it has practical relevance and ransforms (9) into a simple *ordinary* differential equation $w'' + kw = 0$.

Case 1: $k = \lambda^2 > 0$

In this case, function $w = h^{3/2}$ must satisfy the Helmholtz equation (see (9))

$$\nabla^2 w + \lambda^2 w = 0 \tag{11}$$

for (10) to be a (nonhomogeneous) Helmholtz equation in $\mathcal{P}$.

A family of closed-form solutions to (11) is

$$w(x, y) = A_1 e^{i\lambda(\alpha x + \sqrt{1-\alpha^2}\, y)} + A_2 e^{-i\lambda(\alpha x + \sqrt{1-\alpha^2}\, y)} \tag{12}$$

with $0 \le \alpha \le 1$. By taking the real part, we obtain a first family of possible film shapes

$$h_1(x, y) = \{A \sin[\lambda(\alpha x + \sqrt{1-\alpha^2}\, y) + \varphi]\}^{2/3} \tag{13}$$

where A, φ and $\lambda \neq 0$ are constants to be chosen arbitrarily, provided $h_1 > 0$ within the pad. Notice that $\alpha = \cos\vartheta$ defines the direction θ in the xy-plane along which the sine function "develops".

The important case $h = h(x)$ is promptly obtained from (13) by setting $\alpha = 1$, that is $\theta = 0$

$$h_1(x) = [A \sin(\lambda x + \varphi)]^{2/3} \tag{14}$$

It is worth noting that (14) can also be obtained as the general integral of the ordinary differential equation $w'' + \lambda^2 w = 0$ (cfr. (11)), and, therefore, represents *all* possible solutions to this case.

Case 2: $k = 0$

In this case, function $w = h^{3/2}$ must satisfy a Laplace equation (see (9))

$$\nabla^2 w = 0 \tag{15}$$

Possible closed-form solutions to (15) are given by the *harmonic polynomials* $w(x, y) = P_n(x, y)$

$$P_0 = C_0$$
$$P_1 = C_1 x + C_2 y + P_0$$

$$P_2 = C_3(x^2 - y^2) + C_4 xy + P_1$$
$$P_3 = C_5(x^3 - 3xy^2) + C_6(y^3 - 3yx^2) + P_2$$
$$\dots \tag{16}$$

In each P_n, $n > 0$, the two independent terms of degree n can be formally obtained as the real and imaginary parts of $(x + iy)^n$. For example, if $n = 2$, $\Re[(x + iy)^2] = x^2 - y^2$, and $\Im[(x + iy)^2] = xy$.

Notice that any selection of constants C_i is possible. For instance, setting all coefficients with even index equal to zero results in a function symmetric with respect to the x axis (as often encountered in applications).

In general, possible film shapes are given by

$$h_2(x, y) = [P_n(x, y)]^{2/3} \tag{17}$$

provided $P_n > 0$ within the pad bearing Ω.

With $h(x, y)$ as in (17), the Reynolds equation becomes a nonhomogeneous Laplace equation in $\mathcal{P}$ (often called Poisson equation).

For $n = 0$, expression (17) gives simply $h = C_0 = \text{const}$, so that the r.h.s. in Eqs. (1) and (5) is zero, and both equations simply become a homogeneous Laplace equation. Therefore, this well known case, typical of externally pressurized bearings (hydrostatic lubrication [20]), is obtained as just a particular case.

A film profile that varies only in the x-direction is obtained from (16) and (17) by selecting only C_0 and C_1 not equal to zero

$$h_2(x) = [A\,(\beta x + 1)]^{2/3} \tag{18}$$

It is worth noting that (18) represents *all* solutions of the one-dimensional counterpart of (15), that is of the ordinary differential equation $w'' = 0$.

Case 3: $k = -\lambda^2 < 0$

In this case, function $w = h^{3/2}$ has to satisfy the equation (see (9))

$$\nabla^2 w - \lambda^2 w = 0 \tag{19}$$

This is sometimes referred to as the Klein-Gordon equation (or modified Helmholtz equation).

A family of closed-form solutions is given by

$$w(x, y) = A_1 e^{\lambda(\alpha x + \sqrt{1-\alpha^2}\,y)} + A_2 e^{-\lambda(\alpha x + \sqrt{1-\alpha^2}\,y)} \tag{20}$$

with $0 \le \alpha \le 1$. Expression (20) can also be written in a different (though equivalent) form

$$w(x, y) = B_1 \sinh[\lambda\,(\alpha x + \sqrt{1-\alpha^2}\,y)] + B_2 \cosh[\lambda\,(\alpha x + \sqrt{1-\alpha^2}\,y)] \tag{21}$$

where B_1, B_2 and λ are arbitrary constants.

From (21), the following possible film shapes are obtained

$$h_3(x, y) = \{A \sinh[\lambda(\alpha x + \sqrt{1-\alpha^2}\,y) + \varphi]\}^{2/3} \tag{22}$$

$$h_4(x, y) = \{A e^{\pm\lambda\,(\alpha x + \sqrt{1-\alpha^2}\,y)}\}^{2/3} \tag{23}$$

$$h_5(x, y) = \{A \cosh[\lambda(\alpha x + \sqrt{1-\alpha^2}\,y) + \varphi]\}^{2/3} \tag{24}$$

depending on whether $|B_1| > |B_2|$, $B_1 = \pm B_2$, or $|B_1| < |B_2|$, respectively. Of course, the functions within braces have to be > 0 within the pad Ω.

By setting $\alpha = 1$ in expressions (22)–(24), the following film profiles are obtained, which vary only in the x direction

$$h_3(x) = [A \sinh(\lambda x + \varphi)]^{2/3} \tag{25}$$

$$h_4(x) = [A\, e^{\pm\lambda x}]^{2/3} \tag{26}$$

$$h_5(x) = [A \cosh(\lambda x + \varphi)]^{2/3} \tag{27}$$

where the constants A, φ and $\lambda \neq 0$ can be used to fit the required profile (see next Section). Expressions (25)–(27) represent *all* solutions of the ordinary differential equation $w'' - \lambda^2 w = 0$, that is of the one-dimensional counterpart of (19).

For h as in expressions (22) to (27), the Reynolds Eq. (6) becomes a nonhomogeneous Klein-Gordon equation in $\mathcal{P}$.

To the best of the author's knowledge, film shapes like in (13)–(14), (17)–(18), and (22)–(27) (with the exception of the exponential profile), have never been considered in lubrication analysis so far. They appear to form the basis for an effective application of the BEM to self-acting hydrodynamic slider bearings.

4. Analysis of special film profiles

The following analysis is restricted to film profiles depending only on x.

For generality, the bearing length L in the direction of motion has been assumed equal to 1. Therefore, all lengths have to be considered as scaled with respect to the actual bearing length.

Notice, however, that the lubrication problem is still two-dimensional (finite bearing) and the contour Γ may have any shape (Fig. 1, and also Fig. 4).

Since what is relevant is the ratio $h_i/h_o > 1$ between the *inlet* and *outlet* film thickness, it is important to specialize expressions (14), (18), and (25)–(27) to satisfy the conditions (Fig. 1)

$$\begin{cases} h(0) = & h_i \\ h(1) = & h_o \end{cases} \tag{28}$$

Moreover, we will require all wedges to be *convergent*, that is to have $dh/dx \le 0$, for $0 \le x \le 1$. A typical value of the slope in industrial bearings is 0.001 rad, that is 0.06 deg [4, p. 35].

Since expressions (14), (25), and (27) contain three constants and there are only two conditions to be satisfied, λ was used as a parameter. Therefore, λ controls the film shape but does not affect h_i and h_o. Without loss of generality, it is assumed $\lambda > 0$. For brevity, it is convenient to introduce the constants $h_i/h_o = a$ and $(h_o/h_i)^{3/2} = b$. Normal values for a are in the range 2 to 3 [1,2].

To fulfil requirements (28), profile $h_1(x)$ in (14) becomes

$$h_1(x) = h_i \left[\frac{\sin(\lambda x + \varphi)}{\sin\varphi}\right]^{2/3} \tag{29}$$

where

$$\varphi = \arctan\left[\frac{\sin\lambda}{b - \cos\lambda}\right] \tag{30}$$

For profile h_1 to be also monotone in $x \in [0, 1]$, it has to be $0 < \lambda \le \bar{\lambda}$, with $\bar{\lambda} = \arccos(b)$.

Profile h_2 in (18) is always convergent. To have the required inlet and outlet thickness it is necessary that

$$h_2(x) = h_i[(b - 1)x + 1]^{2/3} \tag{31}$$

Profile h_3 in (22) is always convergent as well, and it becomes

$$h_3(x) = h_i \left[\frac{\sinh(\lambda x + \varphi)}{\sinh\varphi}\right]^{2/3} \tag{32}$$

where

$$\varphi = \operatorname{arctanh}\left[\frac{\sinh\lambda}{b - \cosh\lambda}\right] \tag{33}$$

For function h_3 to exist, it is required that $0 < \lambda < \lambda^*$, with $\lambda^* = \ln(1/b)$. For this profile we may also require, for instance, $h_3(0.5) = (h_i + h_o)/2$, so that the profile matches the linear wedge also at the midpoint. The corresponding value of λ is given by

$$\tilde{\lambda} = 2\operatorname{arccosh}\left[\sqrt{2}\,\frac{\left(\frac{1}{a}\right)^{3/2} + 1}{\left(\frac{1}{a} + 1\right)^{3/2}}\right]$$

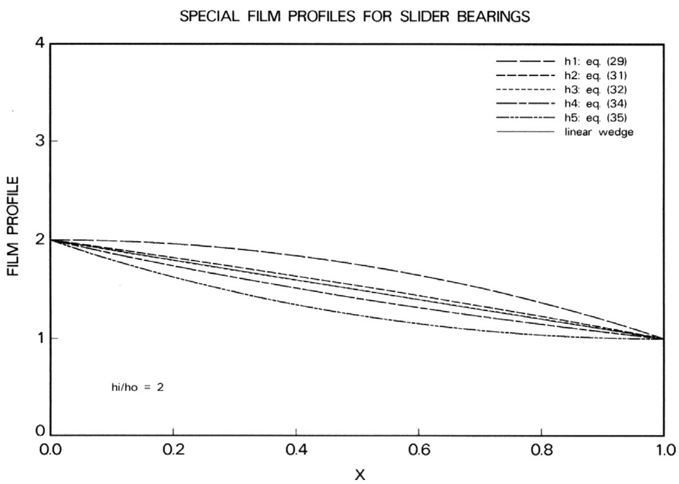

Fig. 2. Special film profiles.

Profile h_4 is always convergent. Its expression is

$$h_4(x) = h_i[e^{\lambda^* x}]^{2/3} = h_i\left(\frac{1}{a}\right)^x \tag{34}$$

Notice that λ has to be equal to λ^*.

Finally, profile h_5 becomes

$$h_5(x) = h_i\left[\frac{\cosh(\lambda x + \varphi)}{\cosh \varphi}\right]^{2/3} \tag{35}$$

where

$$\varphi = \text{arctanh}\left[\frac{b - \cosh \lambda}{\sinh \lambda}\right] \tag{36}$$

For function h_5 to exist and also to be monotone in the interval [0,1], λ must be such that $\lambda^* < \lambda \leq \hat{\lambda}$, where $\hat{\lambda} = \text{arccosh}(1/b)$.

It is worth noting that, in all cases, φ is a function of the ratio $h_i/h_o = a$ and of λ, but not of the actual height of the film, which is only controlled by h_i. Therefore, once the ratio h_i/h_o is fixed, the *shape* of the film (for each type) is controlled only by the value of λ.

Another important feature of the above series of profiles is that, for any $x \in [0, 1]$

$$h_1(x) > h_2(x) > h_3(x) > h_4(x) > h_5(x)$$

so that profiles never intersect. Fig. 2 shows all these special profiles, for the case $h_i/h_o = 2$. The plotted profiles h_1 and h_5 are those corresponding to $\bar{\lambda}$ and $\hat{\lambda}$, respectively, so that they bound the field spanned by *all* (convergent) profiles.

If compared with the linear wedge, film shapes h_1 and h_2 are always *concave*, while h_4 and h_5 are always *convex*. Profile h_3 can be either convex, concave, or have an *inflection point* (at $\bar{x} = [\text{arctanh}(1/\sqrt{3}) - \varphi]/\lambda$) as in Fig. 2, where $\lambda = \tilde{\lambda}$ was used. Notice how closely, in this case, it approximates the linear wedge (also displayed).

Fig. 3 shows the pressure curves associated to the film profiles of Fig. 2 for the case of infinite bearing. Non-dimensional pressure $ph_o^2/(\mu U L)$ is actually used.

From the above observations, and from Figs. 2 and 3, it appears that the proposed series of film profiles covers most of the possible practical cases.

5. Boundary element method for lubrication problems

As already mentioned in Section 3, any of the above profiles enables the boundary element method (BEM) to be effectively applied to the solution of lubrication problems.

Details on the actual implementation of the BEM for linear partial differential equations with constant coefficients like Eq. (10) are now widely available (e.g., [5,6,17]) and are not repeated here for the sake of brevity.

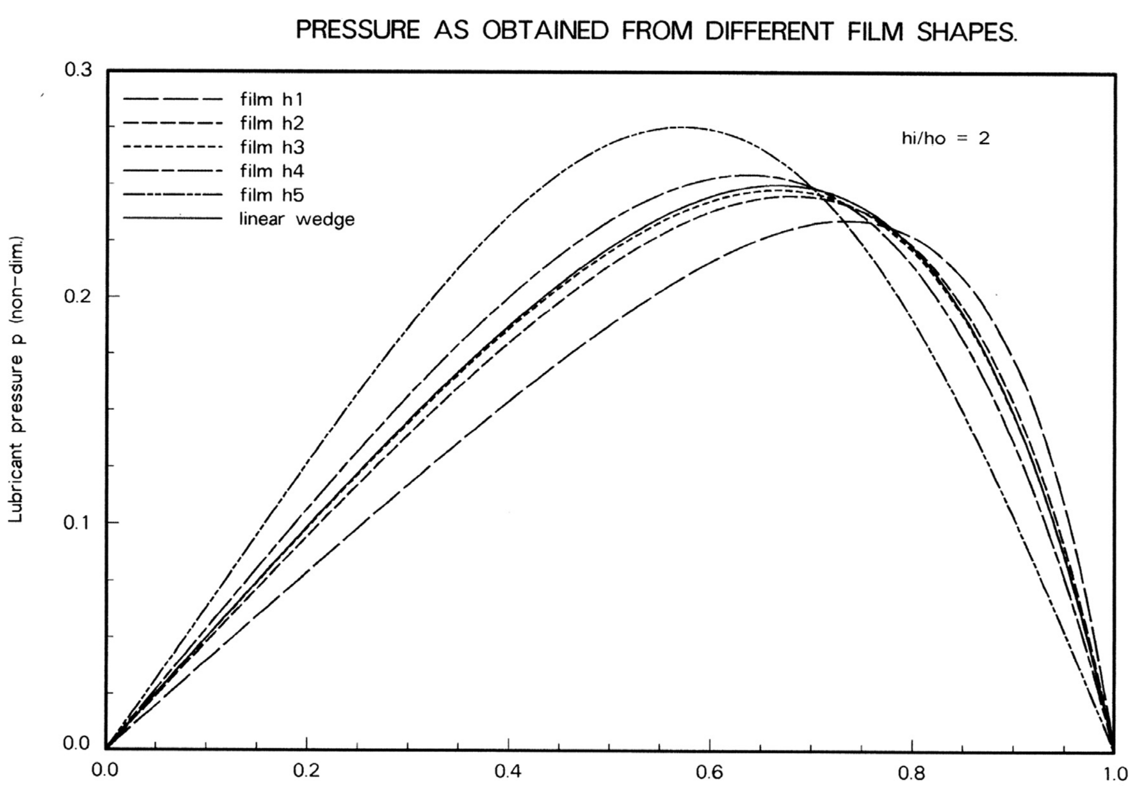

Fig. 3. Pressure curves for infinite bearing ($h_i/h_o = 2$).

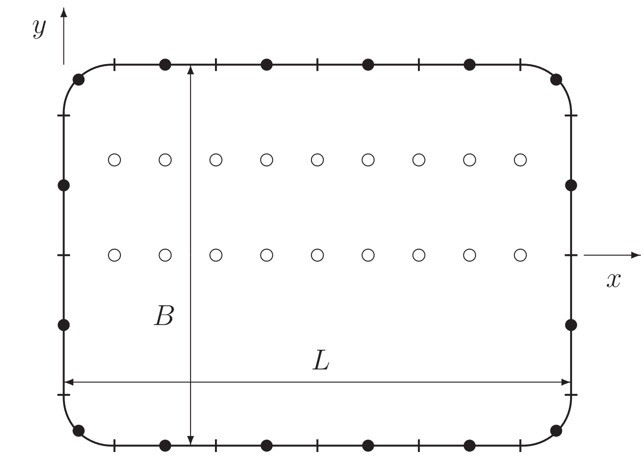

Fig. 4. Finite pad bearing geometry, BEM discretization (|—•—|), and optional internal points (∘).

The BEM is at its best when dealing with problems governed by homogeneous differential equations, while Eq. (10) normally has a nonhomogeneous term $g(x, y)$. Actually, this is not a major drawback, as unknown nodal values are still only on the boundary Γ. However, internal cells may be necessary to integrate some *known* functions on Ω.

In the case of film profiles depending only on x, however, a true *boundary only* approach is possible, as we may write a solution to Eq. (10) in the form

$$\mathcal{P}(x, y) = \mathcal{P}_o(x, y) + \mathcal{P}_p(x) \tag{37}$$

where the *particular integral* $\mathcal{P}_p(x)$ is just a solution of the ordinary differential equation $\mathcal{P}_p'' + k\mathcal{P}_p = g(x)$.

If film profiles $h_2(x)$ (Eq. (18)) or $h_4(x)$ (Eq. (26)) are used (Fig. 2), particular integrals are given, respectively, by

$$\mathcal{P}_p(x) = -(18\mu U / A\beta)\, h_2(x) \tag{38}$$

$$\mathcal{P}_p(x) = \mp(18\mu U / 4\lambda)\, h_4^{-1/2}(x) \tag{39}$$

In the other cases, they may be obtained by any of the one-dimensional methods discussed, e.g., in [3].

The unknown function $\mathcal{P}_o(x, y)$ has only to satisfy the *homogeneous* partial differential equation

$$\nabla^2 \mathcal{P}_o + k\mathcal{P}_o = 0 \tag{40}$$

The associated boundary conditions are immediately obtained from (7)–(8) by replacing $\mathcal{P}$ with $\mathcal{P}_o + \mathcal{P}_p$. For this type of problems, BEM features are fully exploited as only the contour Γ of the bearing pad has to be discretized.

6. Numerical example - finite thrust bearing

In order to test the validity of the proposed approach, a numerical example is reported. The finite bearing pad has a rectangular shape with rounded corners, as shown in Fig. 4. L is the length in the direction of motion, and $B = 0.75L$ is the length normal to the direction of motion. Rounded corners have radius equal to $0.1L$. The pressure p was assumed to vanish on the whole boundary Γ of the pad.

The film thickness was assumed to depend only on x and to be of type $h_2(x)$ (see Eqs. (18) or (31)). The thickness h_i at the leading edge ($x = 0$) and the thickness h_o at the trailing edge ($x = 1$) were in the ratio $h_i/h_o = 2$.

According to the proposed method, the original Reynolds equation in $p(x, y)$ was first transformed into a constant coefficient equation in $\mathcal{P}(x, y)$, that for the selected film shape turned out to be a nonhomogeneous Laplace equation, with boundary conditions $\mathcal{P} = 0$ on all Γ.

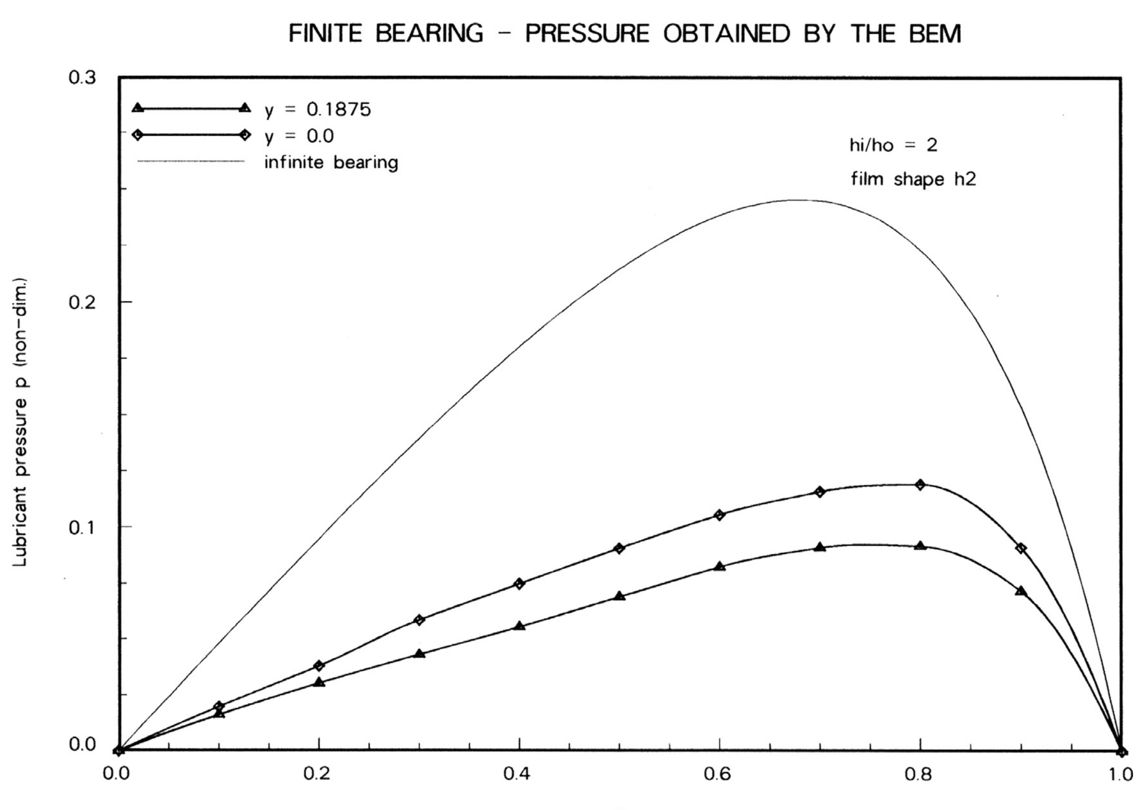

Fig. 5. Finite pad bearing: pressure profiles as obtained by the BEM at selected internal points (see Fig. 4).

Since (38) provided a particular integral $\mathcal{P}_p(x)$ for the transformed equation, the problem was further reduced to a homogeneous Laplace equation $\nabla^2 \mathcal{P}_o = 0$ (see (37)), with boundary conditions $\mathcal{P}_o(x, y) = -\mathcal{P}_p(x)$, $(x, y) \in \Gamma$. The latter was the problem actually solved by the BEM.

Fig. 4 shows the BEM mesh (16 quadratic elements) employed in the calculation. Undoubtedly, it is much simpler than a corresponding FEM mesh.

The BEM solution provides $\mathcal{P}_o$ and $\partial \mathcal{P}_o / \partial n$ all around the boundary Γ.

By using a BEM option, $\mathcal{P}_o$ can also be evaluated at any internal point. Values of the lubricant pressure p are then obtained from the relation $p = (\mathcal{P}_o + \mathcal{P}_p)/h_2^{3/2}$.

Fig. 5 shows the non-dimensional pressure curves obtained along the lines at $y = 0.1875$ and $y = 0$ (Fig. 4).

7. Conclusions

The solution of lubrication problems by the BEM has been discussed in detail. Due to the fact that the Reynolds equation has, in general, variable coefficients, its solution by a true BEM algorithm appeared hardly possible. In fact, it has been shown that there exist several film shapes that allow the Reynolds equation to be easily transformed into a constant coefficient equation, making the BEM application a straightforward task. Most of the proposed profiles closely resemble those actually used in applications. Numerical results for finite bearings confirm the effectiveness of the approach.

Declaration of Competing Interest

None.

References

[1] Pinkus O, Sternlicht B. Theory of hydrodynamic lubrication. McGraw-Hill; 1961.
[2] Cameron A. The principles of lubrication. John Wiley & Sons; 1966.
[3] Szeri AZ, editor. Tribology. Hemisphere Publishing Co.; 1980.
[4] Szeri AZ. Fluid film lubrication. Cambridge University Press; 2011.
[5] Brebbia CA, Telles JCF, Wrobel LC. Boundary element techniques. Springer-Verlag; 1984.
[6] Beskos DE. Boundary element methods in mechanics. North-Holland; 1987.
[7] Clements DL. The boundary element method for linear elliptic equations with variable coefficients. In: Proc. boundary elements X. Southampton, Springer-Verlag; 1988. p. 91–6.
[8] Kelmanson MA. A boundary integral equation method for the study of slow flow in bearings with arbitrary geometries. ASME J Tribol 1984;106:260–4.
[9] Ingham DB, Ritchie JA, Taylor CM. The boundary element method in lubrication analysis. In: Proc. 13th Leeds–Lion symp. on tribology. Leeds, Elsevier; 1986. p. 431–41.
[10] Liu D, Liu YH, Shi XW, Li JY. The finite element and boundary element methods in gas lubrication. In: Proc. int. conf. on tribology. London, IMechE; 1987. p. 53–7.
[11] Khader MS. A generalized integral numerical solution method for lubrication problems. ASME J Tribol 1984;106:255–9.
[12] Xue YK, Gethin DT, Lim CH. Elastohydrodynamic lubrication analysis of layered line contact by the boundary element method. Int J Numer Meth Eng 1996;39:2531–54.
[13] Onsa MH, Sapuan SM, Basri S, Ahmad MMHM, Maleque MA. Elastohydrodynamic lubrication study of hard rolling contact. Ind Lubr Tribol 2001;53:148–54.
[14] Sfantos GK, Aliabadi MH. Boundary element method for elasto-hydrodynamic lubricated multi-body contact. Tribol Lett 2005;20:125–32.
[15] Loeffler CF, Chacaltana JTA, Frasson AMF, Mansur WJa. Simulation of the journal bearing hydrodynamic using two boundary element radial basis interpolation models. Eng Anal Bound Elem 2019;105:188–93.
[16] Cheng AHD. Darcy's flow with variable permeability: a boundary integral solution. Water Resour Res 1984;20(7):980–4.
[17] Rangogni R, Occhi R. Numerical solution of the generalized laplace equation by the boundary element method. Appl Math Modell 1987;11:393–6.
[18] Purday HFP. An introduction to the mechanics of viscous flow. Dover Publ 1949.
[19] Cameron A. Basic lubrication theory. Longman; 1971.
[20] Bassani R, Piccigallo B. Hydrostatic lubrication. Elsevier; 1992.